

Digital particle image velocimetry (DPIV) technique in measurements of granular material flows, Part 2 of 3-converging hoppers

Irena Sielamowicz^{a,*}, Sławomir Błoński^b, Tomasz A. Kowalewski^b

^aTechnical University in Białystok, ul Wiejska 45, Białystok, Poland

^bInstitute of Fundamental Technological Research, Polish Academy of Sciences (IPPT PAN), PL 00-049 Warsaw, Swietokrzyska 21, Poland

Received 30 August 2005; received in revised form 27 February 2006; accepted 2 March 2006

Available online 10 March 2006

Abstract

The flow evolution of an amaranth seed is being investigated in a wedge-shaped model made of Plexiglas. The objective of this paper is to recognise flow patterns in the flowing material, and also to depict evolution of velocity fields, flow field discontinuities, velocity profiles for cross-sections of the model, shear zones and flow streamlines using the digital particle image velocimetry (DPIV) optical technique. It is demonstrated that the DPIV technique used in the experiments enables quantitative analysis of the flow zones geometry. The technique also allows to reveal boundaries between flowing and stagnant zones and to extract velocity profiles at any selected sections of the model.

© 2006 Elsevier Ltd. All rights reserved.

Keywords: Optical technique; DPIV; Granular material flows; Converging hopper; Particle; Plug flow; Shear zones; Discharge flow rate

1. Introduction

The basic assumptions introduced by Jenike (1961, 1964) and Johanson and Jenike (1962) on the radial stress and velocity fields in flowing of granular materials have been used by many engineers in their theoretical and experimental works. Numerous theoretical expressions are derived for velocity distributions in a granular material discharging from converging hoppers like wedge-shaped or conical.

In the theoretical models of granular flow, the assumption of incompressibility throughout the hopper is an essential element in the predictions of velocities and flow boundaries. The mathematical models introduced into the analyses assume a rigid-perfectly plastic model (Hill, 1950; Prager and Hodge, 1968; Salençon, 1977) or purely kinematic material model, as proposed by Litwiniszyn (1963). It was further developed by Mullins (1972, 1979) and applied by Nedderman and Tüzün (1979), Tüzün et al. (1982), Waters and Drescher (2000), or in a revised form by Drescher and Ferjani (2004). Nedderman (1995) presented a theoretical model for an unsteady process of discharge, based on the incompressible radial velocity field

resulting from the kinematic theory. There are also analytical approximate methods applied in the analysis of hopper loads and hopper geometry design like the limit state methods, the methods of differential slices, and the method of plastic limit analysis, Drescher (1991).

The use of the PIV technique for granular flows was presented by Lueptow et al. (2000). The authors recommended an application of PIV to study quasi-two dimensional flows in transparent containers. The classical PIV technique uses a direct or FFT-based cross-correlation of two sequential flow images. Evaluation of the correlation's peak and estimation of its location in the image plane reveals a mean displacement of the flowing material. It is obtained for each interrogated image sections. By using known time intervals between correlated images, a mean velocity vector can be calculated. The method is quite sensitive to the image partitioning, seeding uniformity, and correct matching of section's sizes to time intervals between correlated images. Digital particle image velocimetry (DPIV) based on the optical flow (OF) approach may use several images of the sequence. The OF-DPIV algorithm seeks geometrical transformations, which match intensity patterns of the images in an iterative manner. Having these transformations, displacements are evaluated directly for each image pixel. The achieved accuracy of measured displacements is about 0.5 pixel for an

* Corresponding author. Tel.: +48 85 7469583; fax: +48 85 7469559.

E-mail addresses: sielirena@pb.bialystok.pl (I. Sielamowicz), sbloński@ippt.gov.pl (S. Błoński), tkowale@ippt.gov.pl (T.A. Kowalewski).

evaluation procedure with two-image sequences and 0.2 pixel for three-image sequences (Quenot et al., 1998). More details about the OF-DPIV technique can be found in Quenot et al. (1998), where a significant increase in the accuracy and spatial resolution of the evaluated velocity fields is demonstrated.

As it was recently reported by Steingart and Evans (2005), Sielamowicz et al. (2005), an application of DPIV technique to granular flows in two-dimensional hoppers appears to be very promising. Despite its limitations (only flow close to the transparent wall is observed), DPIV technique offers unique possibility to obtain full field transient velocity fields, and, by applying standard mechanical relations, offers possibility to evaluate distribution of shear stresses in the material.

Here, we use OF-DPIV technique to obtain experimental data on evolution of the converging granular flow in a wedge-shaped hopper model. This novel optical technique allows us to measure a velocity field in the vicinity of the transparent front wall of the model. Velocity vector fields, flow profiles, and geometrical characteristics of the granular material flowing in the Plexiglas model are assessed.

2. Theory and experiments in converging hoppers

Experimental investigations of flow patterns in converging hoppers have been presented in numerous publications, e.g. Pariseau (1969), Blair-Fish and Bransby (1973), Lee et al. (1974), Nguyen et al. (1979), Tüzün and Nedderman (1982), Langston et al. (1996, 1997), Ooi et al. (1998). Pitman (1986) investigated stress and velocity fields in two- and three-dimensional hoppers. To investigate granular flows in laboratory models special techniques were used as X-ray pictures, ultrasonic measurement, transparent walls. Kvapil (1959) used two different colours of investigated material to detect the zones of flow and the stagnant zones. Drescher et al. (1978) presented experiments in a plane parallel/converging bunker using a stereo-photographic technique. Dosekun (1980) measured the granular material flow in a wedge-shaped hopper with transparent walls. Also, other non-invasive measurement techniques were applied to register granular flows, density and velocity fields in flowing zones, among others spy-holes, radio transmitters, positron emission (Ooi et al., 1998), magnetic resonance imaging, radioactive tracers, and ultrasonic speckle velocimetry. More details on different techniques used in investigations of granular flow in small models can be found in references given by Ooi et al. (1998) and by Lueptow et al. (2000). Insightful experimental investigations devoted to granular flow in conical hoppers are reported in literature, among others, by Nedderman (1988), Moreea and Nedderman (1996). Most of above-mentioned experiments are made in models. Due to difficulties in monitoring of granular flow through opaque walls there are only a few full scale experimental investigations reported in silos. It is worth it to mention Ooi et al. (1998), who presented full scale measurements of flow patterns in a gypsum silo.

In spite of the fact that results obtained from theoretical models may appear uncertain, researchers are still looking for a better way to recognise flow patterns using models and to pre-

dict the flow mode of the material stored in the hopper. The flow patterns occurring in the hopper have a strong influence on wall pressure, strongly depend on silo geometry and granular material properties. They may vary in a non-linear manner according to the stress state which is quite different in a model and in a full scale hopper. The stress state varies consequently with different flow patterns, usually being different in model investigations and full scale hoppers. Therefore, the experimental validation of theoretical models appears to be a very necessary task.

Investigations concerning stress and velocity fields reported by Jenike (1961, 1964), Johanson and Jenike (1962), gave evidence that for plane strain and axial symmetry, the stress field requires a solution in a form of a system of two hyperbolic partial differential equations. The velocity field could then be computed by solving another system of two linear homogeneous partial differential equations of the hyperbolic type. The radial stress field is assumed to be particularly important for straight conical channels, because evidence was presented elsewhere that all general fields tend to approach the radial stress fields in the vicinity of the vertex. These ideas were further developed by several researches like Horne and Nedderman (1978), Pitman (1986), Cleaver and Nedderman (1993a,b), Drescher (1991).

Tüzün et al. (1982) presented a review article with all the experimental methods that were used to measure velocities in a granular material. The paper also considered extension of the plasticity theory, well established for the predictions of small displacements in granular materials, to the effectively infinite strains found in flowing systems. This was compared with the alternative methods of predicting velocity distributions based on the kinematic or stress free models of Litwiniszyn (1963) and Mullins (1972). The details of experimental measurements of velocity distributions and comparisons with the theoretical predictions were presented. In the review article, Tüzün et al. (1982) discussed both two- and three-dimensional flows and both wedge-shaped and conical hoppers. Later, the measurement techniques of flows and theoretical approaches were developed. Although other authors reported the existence of discontinuities in velocity fields, a series of X-ray pictures and ultrasonic measurements presented practically uniform density of the flowing material. In most of the theoretical models the velocity field analysis was restricted to the advanced stage of the flow, which was treated as a pseudo-steady process. A theoretical description of the kinematics of the advanced phase of the flow is based on the plane plastic flow theory of an incompressible material coupled with the radial stress field. It reveals realistic velocity field, particularly in hoppers with smooth walls. A similar strategy of solving kinematics in hoppers was proposed by Pariseau (1969). Drescher et al. (1978) presented experimental results of flow patterns in a plane, wedge-shaped hopper, and also an approach to a theoretical description of discharge. A non-steady discontinuous velocity field was measured using a stereo photographic technique.

Stress and velocity fields in two- and three-dimensional hoppers were also considered in the steady-state flow of an incompressible, cohesionless granular material by Pitman (1986). He presented a numerical method for solving the equations

governing the flow of a granular material, extending his solution to three-dimensional hoppers. Polderman et al. (1985) proposed a calculation method which gave a good prediction for the velocity distribution in mass flow hoppers (wedge-shaped and conical). The method was based on the classical plasticity theory. The results given in Polderman et al. (1985) supported the assumptions about the distribution of the stress components made by Walker's differential slice model (1966). Nedderman (1988) presented a new technique for measuring the velocity distributions in conical hoppers. Marker particles were released in the already-flowing material. The velocity distributions were deduced from the measured times of passage. A minor effect of the size and density of the marker particles was shown and the velocity of these particles adequately represent the velocity of granular material. The theoretical predictions given by Johanson and Jenike (1962), and among others by Mróz and Szymański (1971), were reviewed and two original modifications were presented. The method introduced by Nedderman (1988) showed that the marker particles move with the same velocity as the surrounding material and this assumption was confirmed by the experimental results. The only small dependence of the time of passage on the size and density of the marker particles showed that there was no need to match the marker and bulk particles closely. By integrating the velocity profiles, the flow rate was calculated. It proved a good agreement with the flow rate measured independently, giving confidence in the accuracy of the method. Theoretical predictions made for granular flow in wedge-shaped hoppers do not give a satisfactory approach to the radial stress and velocity fields. Calculations in conical geometries only appeared successful for either materials of unrealistic angles of friction, or for circumstances in which the stresses at the top surface were close to those predicted by the radial stress field. Experiments reported by Cleaver and Nedderman (1993a,b) showed that the velocities in the lower half of a conical hopper are radial with magnitudes similar to those predicted from the radial velocity field. Moreea and Nedderman (1996) used the method of characteristics to predict the exact stress and velocity fields in an incompressible, cohesionless Coulomb material discharging from a conical hopper for a great variety of boundary conditions imposed on the upper surface. They found that in all cases, stress and velocity tend to approach the radial stress and velocity fields, and that convergence was achieved about half way down the hopper. The velocity fields show the regions of more or less constant velocity separated by velocity discontinuities. This statement made by Moreea and Nedderman (1996) justified the assumption in Drescher's (1991) method of predicting velocity distributions. Watson and Rotter (1996) used the finite element analysis to calculate the steady-state velocity in a cohesionless granular material discharging from a planar flat-bottomed silo. The relationship between the horizontal velocity and the horizontal gradient of the vertical velocity was the basic assumption in the analysis. Langston et al. (1996) investigated two-phase flow of interstitial air in a moving bed of granular solids in a mass flow hopper. Langston et al. (1997) compared DEM simulation of granular material flows in two- and three-dimensional hoppers to imaging data from conven-

tional photography and gamma-ray tomography. Deformation rate, velocity fields, and stress distributions were calculated in a model of converging silo by Böhrnsen et al. (2004), who used the finite element method based on the Euler's reference frame. The flow profiles were investigated and the stress evolution was obtained, e.g., a stress alteration on the way from the outlet for the conical and the cylindrical section of the silo. The focus of this paper is to elucidate the character of the flow in converging models. It demonstrates the ability of the novel DPIV technique to measure velocity fields for the cohesionless granular material flowing in wedge-shaped hoppers and to obtain quantitative data on the flow evolution.

3. Experimental procedure

Experiments described in the paper were conducted in a plane converging model made of Plexiglas. Fig. 1 presents a schematic view of the experimental setup. The model wall has a shape of a isosceles triangle with the height 80 cm. The depth of the model is 10 cm with a value of inclination of the walls to the vertical 30° . The length of the upper edge of the wall is about 104 cm. The lower vertex of the triangle was cut off to form an 1 cm broad outlet. Below the outlet a granular material was collected to the box and reused in next experiments. The model was placed on a metal rig. Our flow analysis was limited to the area above the bottom Plexiglas box attached above the outlet (comp. Fig. 4). Its position defines our "bottom line", i.e., beginning of the coordinate system used in the following to describe measured velocity fields. The granular material was supplied through a pipe fixed in a box suspended above the model. The box is a round plastic vessel of 5 l volume. The vessel is 16 cm of height and of radius 10 cm. The pipe was vertically located 5 cm below the upper edge in the model. Uniform and repeatable packing of the material with no particle segregation was obtained.

The granular flow evolution was recorded using a high-resolution CCD camera (2048×1536 pixels). The experimental setup permitted to acquire a series of about 200 short

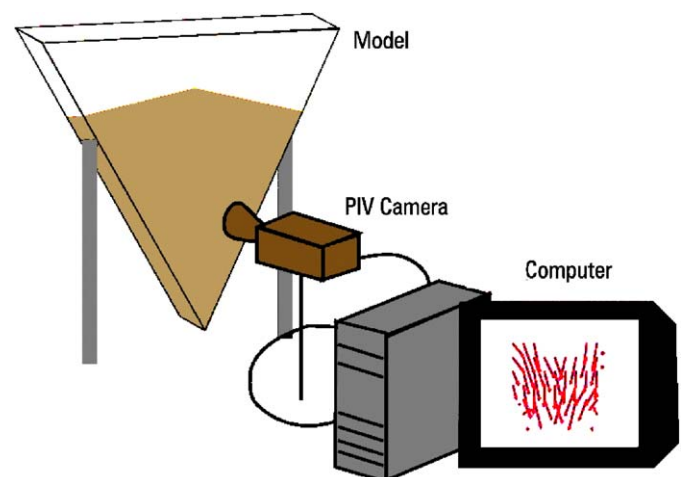


Fig. 1. Experimental setup.

Table 1
Material properties of the seeds used in the experiments

Granular material	Wall friction against Plexiglas	Angle of internal friction	Granular material density deposited through a pipe with zero free-fall	Granular material density at 50 cm free-fall
	φ_w (deg.)	φ_e (deg.)	ρ_b (kg/m ³)	φ_b (kg/m ³)
Amaranth	25	28	810	890

exposure images and store them on the computer disk. After experiments were done, computer files containing images of the flow were used for the velocity evaluation. Illumination with several fluorescent lamps allowed to obtain shadow-free images of the amaranth seed filling the model. The flow was observed in back-scattered light through a transparent front wall of the model. Time interval between images was kept constant, equal to 1.05 s, selected as an optimal value allowing to detect the smallest seed displacements in the flow. The seed displacements measured for the given time interval delivered local velocity vectors. Pairs or triplets of digital images were taken to assess by the OF-DPIV method velocity field in the flowing material.

Amaranth seed was used as the granular material in the experiments. It developed negligible static electricity when flowing and sliding over Plexiglas. Main properties of the granular material used in the experiments are given in Table 1.

To present more material's properties the angle of internal friction of densely packed material was measured and it varied from $\varphi_e = 40^\circ$ at normal stresses 3.8 kPa to $\varphi_e = 31^\circ$ at normal stresses 21.6 kPa.

The value of the angle of internal friction given in Table 1 is taken from the Polish Standard. The value of wall friction against Plexiglas was determined experimentally. Moisture of the grains was found as 10.2%. Granular material density was also measured in two cases with zero-free fall.

The model was filled with 60 cm high column of amaranth seed. Vertical orientation of the model was carefully checked to avoid any disturbance of the flow symmetry. Before each experiment the discharge rate was measured every 30 s with a digital scale. Reproducibility of the discharge process was very good, allowing to assume that the same discharge level is suitable to describe recorded flow images.

4. Experimental results

Upon opening the outlet, the material sets in motion and a narrow plug flow zone propagates upward. The material moves into the flowing zone from the upper parts in an avalanche manner. In fact, there is a flow channel formed at the symmetry axis. In the lower parts the boundaries of the flow region are almost vertical, at higher levels the flowing zone widens and finally reaches the walls of the model. The velocity vectors in the upper part of the flowing material are directed radially to the flow channel and the assumption of Jenike radial flow is here confirmed. In the flow zone velocity vectors are mostly vertical, placed along the flow channel.

The formation of a narrow plug flow zone and its propagation upward during the discharge process is quantitatively evaluated. This effect is associated with another interesting phenomenon of the flow—as shear zones and discontinuities of vector fields. It is found that the size of the observed flow region increases with time and shear zones occur between the flowing and stagnant material. These shear boundaries are partly vertical and they have a form of “steps”. The flowing zone widens and the evolution of “the shear steps” boundaries is shown in the consecutive time steps of the flow. The density of the flowing material is distinctly lower than in the surrounding material packed in the stagnant zones. It can also be found in the velocity magnitude contours obtained for models with vertical walls, as it was reported by Ostendorf and Schwedes (2004), Sielamowicz and Kowalewski (2004) and Sielamowicz et al. (2005).

The material, after filling, formed the upper free surface of a constant slope at an angle equal to the material's angle of repose. With progressing discharge the upper surface lowers and changes its shape. The evolution of the upper surface for flowing amaranth seed is shown in Fig. 2. The left column of Fig. 2 presents vector fields evaluated for the flowing material by DPIV method. It is seen that the width of the plug flow zone increases rapidly. Only near the walls the narrow stagnant zones can be observed. The boundaries between the flow region and the stagnant zones are observed in a form of “stairs”. This observation relates to shear zones occurred between the flow region and the stagnant zones. The shear zones in the flowing material are further presented in Fig. 3. The points denote velocities equal zero, regions of material stagnation. The vectors located near the upper surface are directed towards the flow region, indicating radial direction of the flow. The depicted vector fields indicate that instantaneous velocities at various locations of the flow region appear to be nearly vertical and constant within this region and that the mean velocity (length of the vectors) decreases with time.

In the right column of Fig. 2, evolution of the upper surface of flowing amaranthus' seed is shown. Just after opening the outlet, one can observe the development of a channel of the flow, where the material's density becomes rapidly lower than in the surrounding material. Some strongly asymmetric, local behaviours and avalanche mode of the flow can be observed in the vector fields. Although filling of the model is symmetric, the material flow is not in fully symmetric. This fact may be caused due misalignment of the model. Disparity of the material flow from the left or the right wall into the flow channel creates sloshing motions. These sloshing motions give evidence of flow instabilities generated by dynamic changes of the material's density and variations in the material's friction coefficient.

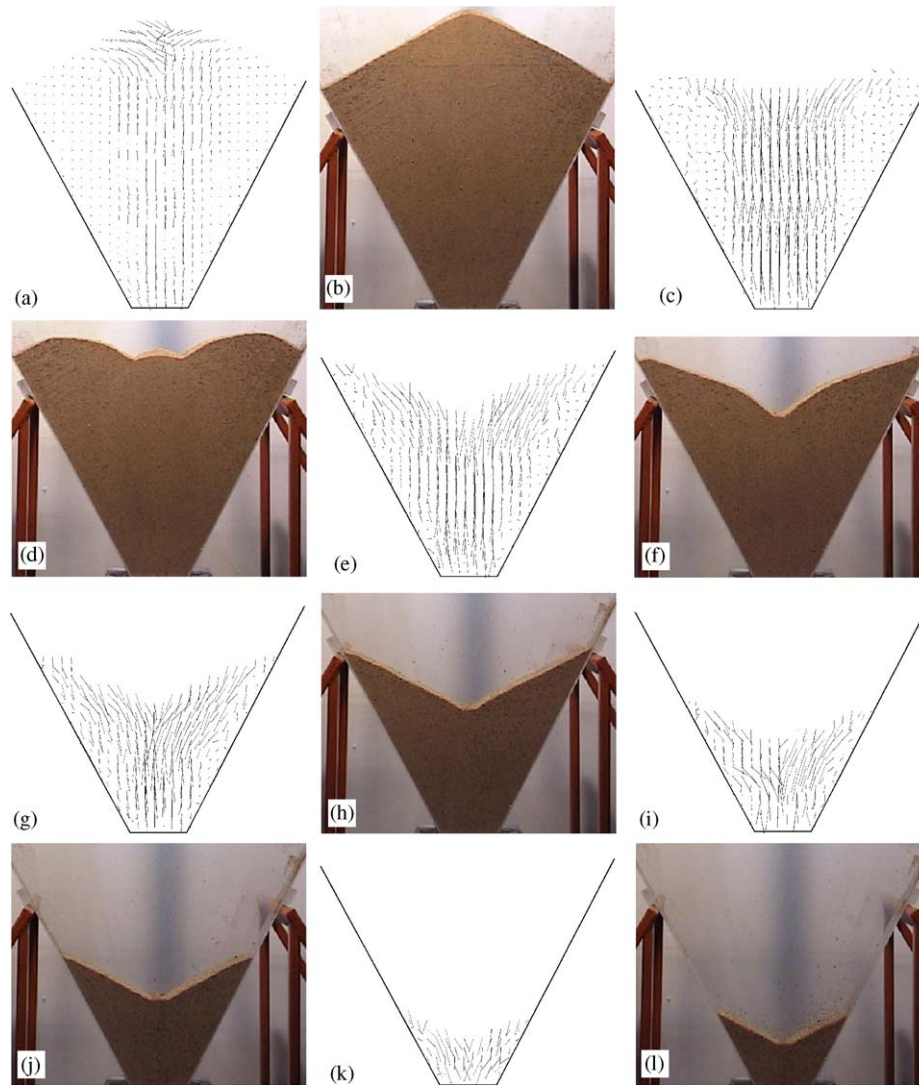


Fig. 2. DPIV evaluated velocity vector fields (left column) and observed evolution of the upper surface in flowing amaranth seed (right column) for six time steps: 7 s, 45 s, 95 s, 120 s, 180 s and 241 s after opening the outlet.

As the time of the flow elapses, the flow region broadens and finally almost the whole material is in motion. In the flow region vectors are directed vertically to the outlet, radial flow component is present only in the avalanche part of the flow in vicinity of the surface.

The observed vector field reveals two different flow regions. One is visible in the radial avalanche flow mode and the other is represented by the uniform channel flow in the vertical direction. Such state of flow exists till 120 s of the flow. Then, because there is less and less material in the model, the radial velocity field connects to the vertical vector field. A curved boundary indicating rapid changes in the flow direction can be identified in the vector field. In the subsequent flow time both regions merge and only the radial velocity field is observed.

Fig. 3 presents velocity and streamlines measured in the flowing amaranthus' seed in the initial phase of the flow, at 45, 95 and 195 s of the flow time. To depict transient development of different flow regions, the velocity vector field is overlaid with contours of the velocity magnitude in Fig. 3 (left column).

The right column of Fig. 3 shows flow streamlines, i.e., flow paths obtained by integrating DPIV velocity vector field. In Sielamowicz et al. (2005) a term “trace of selected particles” was introduced instead of streamlines. However, it should be noted that these lines do not represent paths of individual particles, but rather indicate instantaneous motion of the bulk material.

It can be seen that initially (Fig. 3a–d) the vertical channel of the high velocity region develops in the middle part of the flowing material and it propagates quickly upward. Its shape does not change much with time. Only after reaching the free surface it starts to propagate down, into the inlet. The shape of the vertical channel is almost the same in the whole analysed flow time. Fig. 3b, d, f show that in the flow region located in the middle part of the model material moves nearly vertically to the outlet. The radial velocity field is visible only in the upper part of the flowing material, where the avalanche type of flow develops. It is indicated by curvature of streamlines near the upper surface (Fig. 3b, d, f). After 120 s the flow velocity

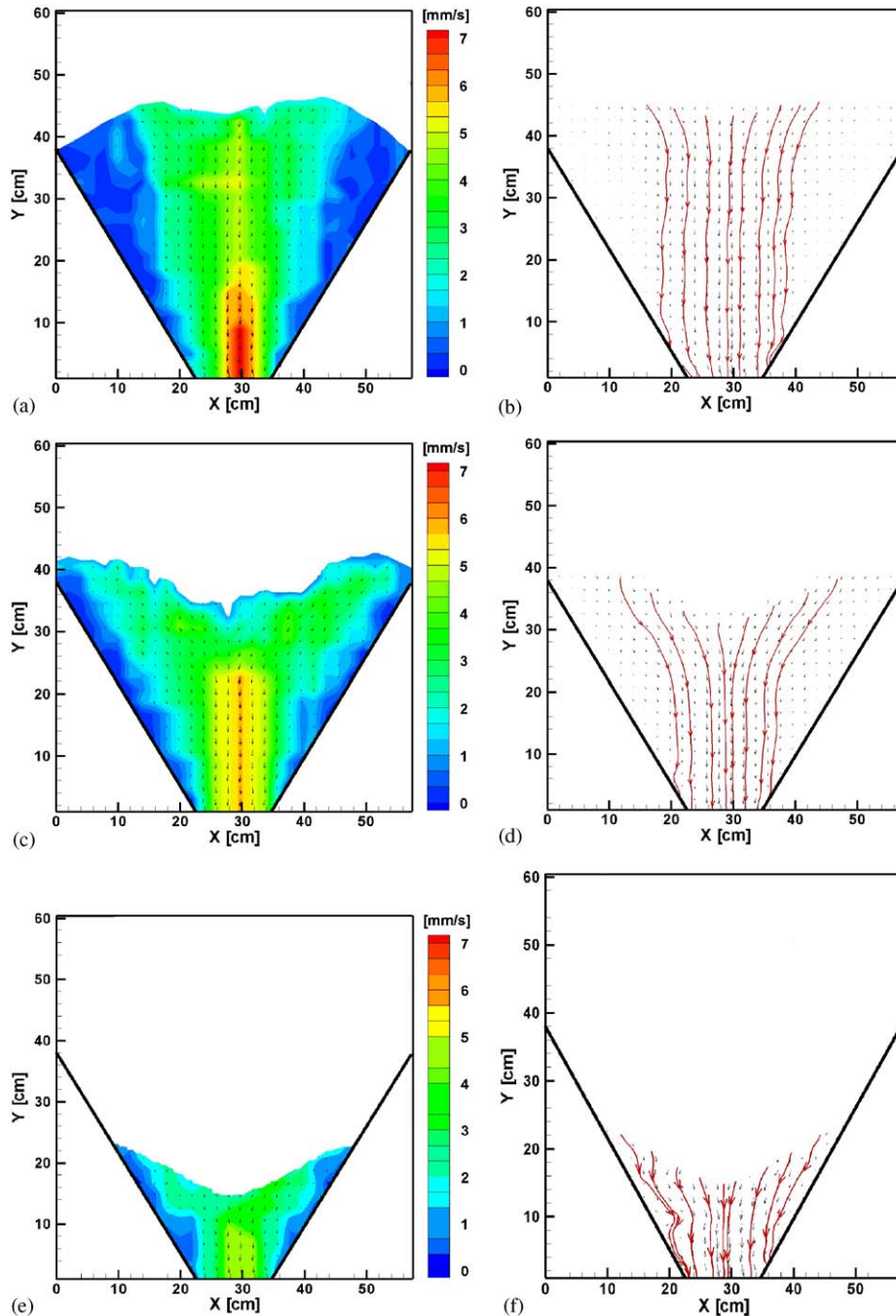


Fig. 3. Flow velocity vector field and velocity magnitude contours in the flowing amaranth seed (left column); flow streamlines calculated from the velocity field (right column), evaluated for three time steps 45 s, 95 s and 195 s after opening the outlet.

decreases (comp. velocity contours in Fig. 3a, c, e). Some asymmetry of the flow pattern can be noticed. These local phenomena is better visible in the velocity profiles shown in Fig. 3.

Full field velocity measurements allow to extract velocity profiles at selected cross-section of the model. It helps to identify shape of the flow channel and to make quantitative comparison of different flow regimes. Three horizontal cross-sections have been selected for such analysis: $H = 19, 38, 57$ cm, from the beginning of our coordinate system, i.e., above the bottom line shown in Fig. 4. It corresponds approximately to 0.41, 0.67,

and 0.94 of the initial material height. Fig. 4 shows location of the selected levels in the model.

Below in Figs. 5–12 we present profiles of the vertical velocity component V_y extracted across the channel from appropriate vector fields. Negative velocity values indicate flow direction down to the bottom. After extracting the velocity values the curves are smoothed using cubic-spline method. It may create small artefacts, especially close to the walls and at the flow axis, where strong velocity gradients are present. On the other hand, smoothed profiles are necessary to

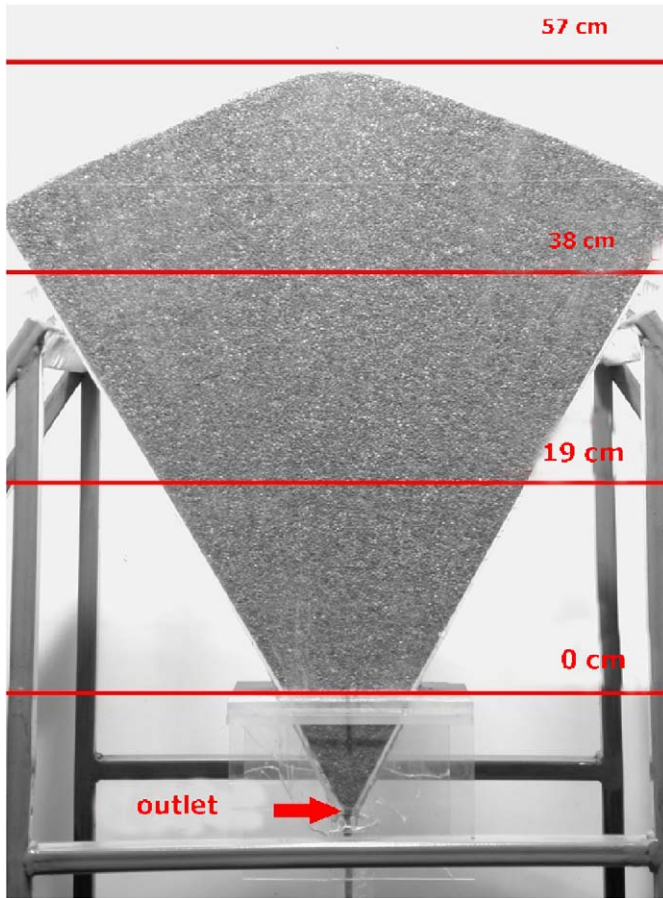


Fig. 4. Location of the selected cross-sections used to evaluate the velocity profiles: $H = 19, 38,$ and 57 cm from the bottom line ($H = 0$ cm) of the model. Elapsed flow time is 10 s.

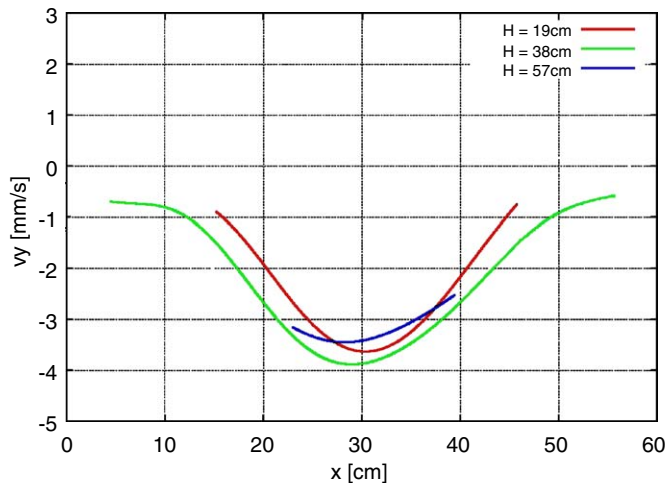


Fig. 5. Vertical velocity component measured across the channel at $H = 19, 38,$ and 57 cm. Time step $t = 7$ s after opening the outlet.

compare them at different time steps and to detect asymmetry of the flow.

It is worth noting that material is removed from the model as time passes. Hence, depending on the time step and the

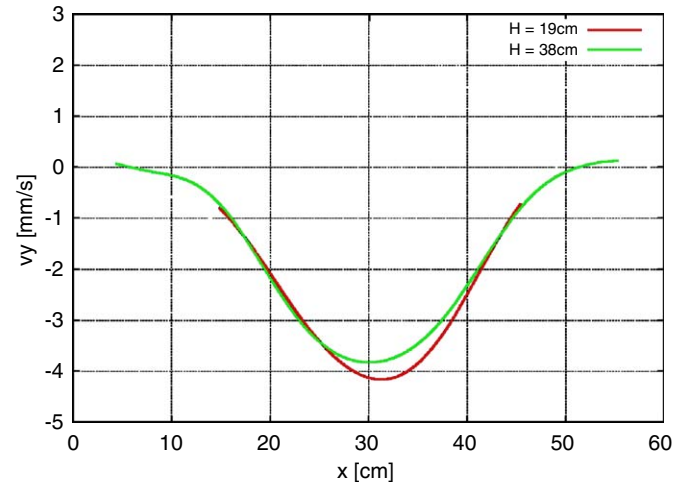


Fig. 6. Vertical velocity component measured across the channel at $H = 19$ and 38 cm. Time step $t = 23$ s after opening the outlet.

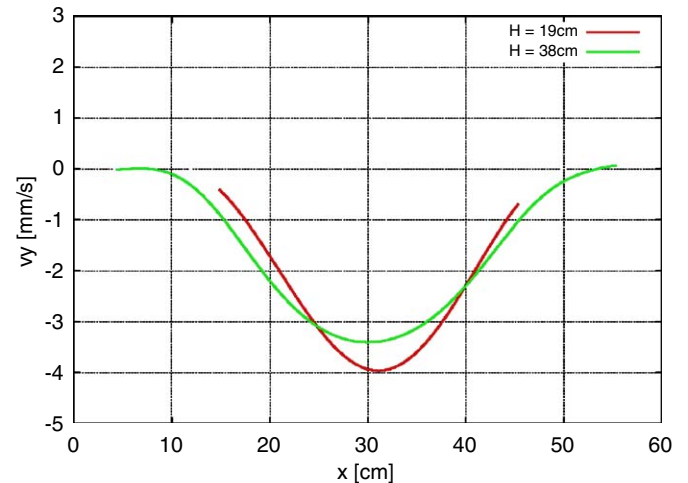


Fig. 7. Vertical velocity component measured across the channel at $H = 19$ and 38 cm, from the bottom. Time step $t = 45$ s after opening the outlet.

profile location, only part of the model is filled with the seed. Therefore, some velocity profiles shown in the figures exhibit broken lines or they disappear at later time steps.

Fig. 5 shows velocity profiles extracted from DPIV vector field evaluated at the time step $t = 7$ s. It is the first analysed moment of the flow. As it is seen in Fig. 4 the highest location ($H = 57$ cm) is partly filled with the seed and only a short section of the profile is shown in Fig. 5. Nevertheless, the initial asymmetry of the flow is clearly visible, indicating beginning of the sloshing motion for the avalanche flow regime at the surface. This asymmetry is present for the mid-height profile ($H = 38$ cm) too, but it almost disappears at the bottom ($H = 19$ cm). It means that when the material starts to flow, not only the plug flow zone develops but a slight lateral motion of the packed material is present from very beginning as well. By comparing maxims of the velocity one may find that the plug flow slightly accelerates for the mid-height ($H = 38$ cm), and

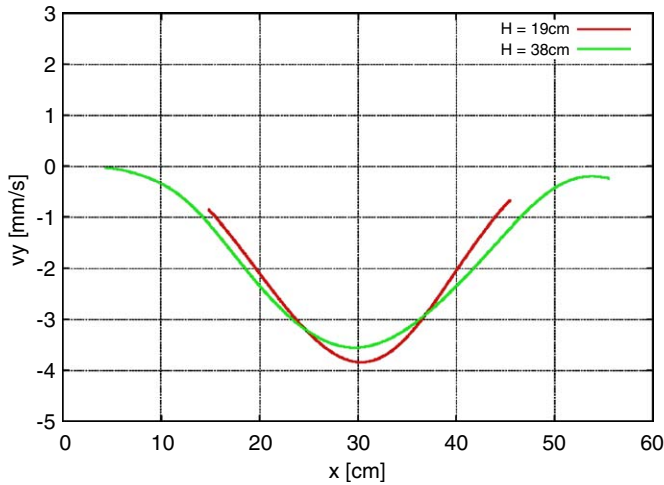


Fig. 8. Vertical velocity component measured across the channel at $H = 19$ and 38 cm. Time step $t = 53$ s after opening the outlet.

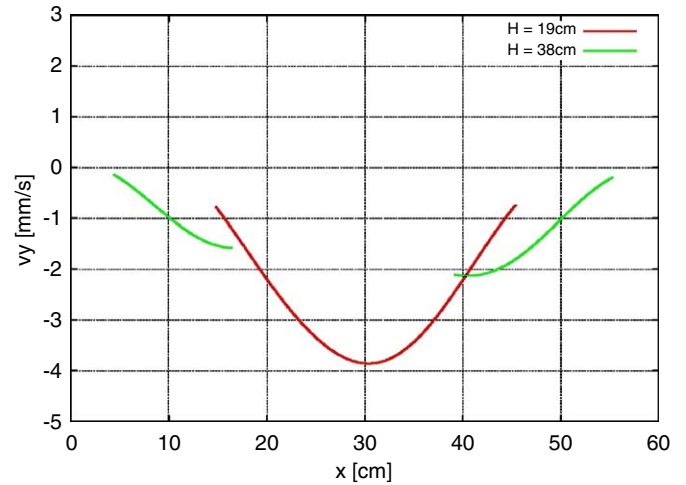


Fig. 10. Vertical velocity component measured across the channel at $H = 19$ and 38 cm, from the bottom. Time step $t = 87$ s after opening the outlet.

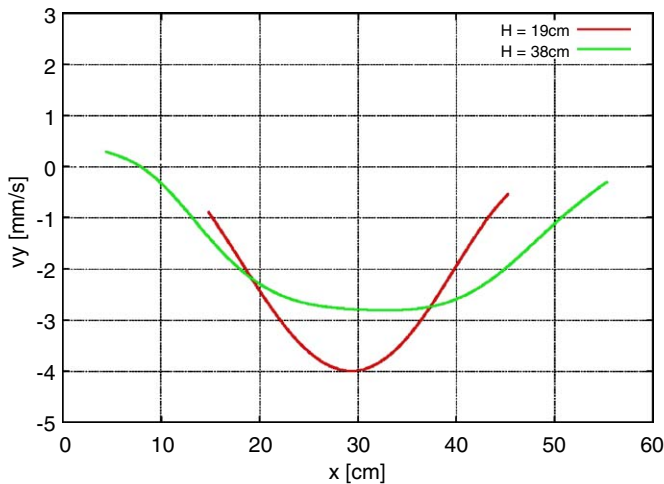


Fig. 9. Vertical velocity component measured across the channel at $H = 19$ and 38 cm, from the bottom. Time step $t = 70$ s after opening the outlet.

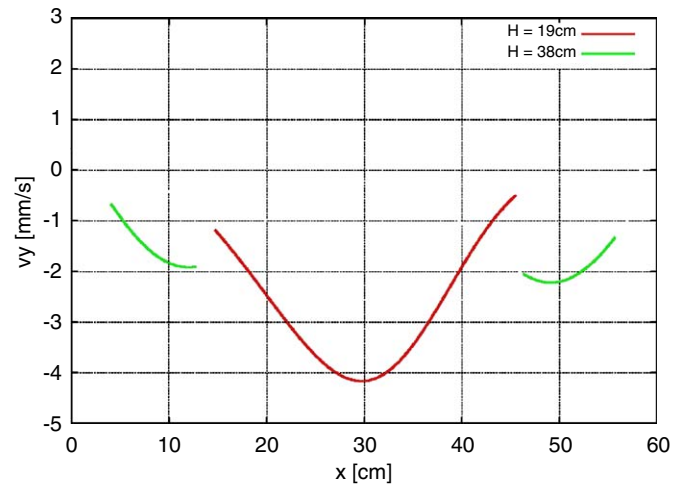


Fig. 11. Vertical velocity component measured across the channel at $H = 19$ and 38 cm. Time step $t = 107$ s after opening the outlet.

decelerates closer to the bottom ($H = 19$ cm). Its value varies from 3.5 to 4 mm/s.

Fig. 6 presents velocity profiles obtained at the later time step $t = 23$ s. Only two locations are filled with the seed: $H = 19$ and 38 cm. The plug flow is well developed and velocity profiles at both locations nearly overlap. The maximum vertical velocity (4 mm/s) is similar to that measured for the earlier time step (Fig. 5). Initial asymmetry of the flow observed in Fig. 5 smoothed out for the mid-profile ($H = 38$ cm), but apparently appeared at the lower location now.

Fig. 7 shows the velocity profiles extracted at the time step of 45 s. As expected in converging models, the flow is nearly symmetrical for the higher level, but the asymmetry near the bottom developed earlier (Fig. 6) remains. Velocity distribution at $H = 19$ cm relates to the narrower flow region than at the location $H = 38$ cm, where the flow region is considerably wider. Whereas maximum velocity at the lower level ($H = 19$ cm) remains constant (4 mm/s), at the higher location the

vertical velocity component evidently diminishes now and its maximum value at $H = 38$ cm is 3.3 mm/s.

The transient change of the converging flow can be observed during the consecutive stages of the flow. The profiles depicted at the time step $t = 53$ s (Fig. 8) indicate slight decrease of the plug flow velocity and further smoothing of the asymmetry present before. These nearly uniform plug flow mode suddenly changes for the next time step (70 s) as it is shown in Fig. 9. In the upper region the avalanche type flow dominates now. The value of the vertical velocity component is higher for $H = 19$ cm and much lower for $H = 38$ cm. Comparing to Fig. 8 where the vertical velocity component for two analysed levels has almost the same values, now velocities for $H = 38$ cm rapidly diminish. This type of flow regenerates flow asymmetry at the upper surface.

The next two figures of the sequence (Figs. 10, 11) show velocity profiles in the material after a funnel-like void area developed at the model axis (comp. Fig. 2f, h). Only small

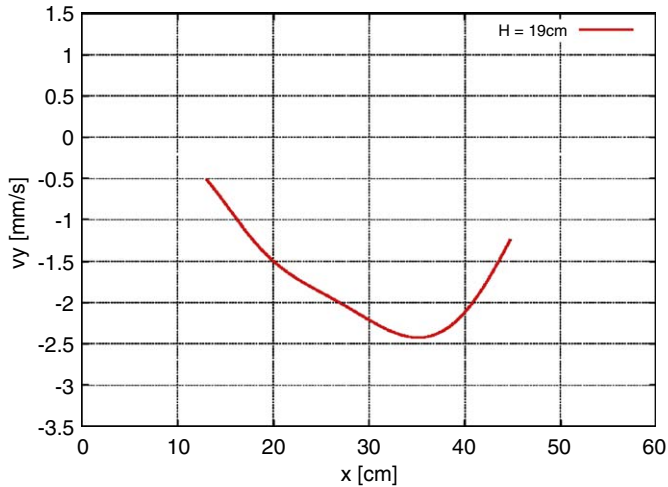


Fig. 12. Vertical velocity component measured across the channel at $H = 19$ cm. Time step $t = 154$ s after opening the outlet.

regions close to the side walls are filled with the seed at the upper level ($H = 38$ cm). The avalanche type flow is mainly parallel to the walls, hence its vertical velocity component evidently diminished. It is evident in the profiles shown for the level $H = 38$ cm (Figs. 10, 11). It is worth noting that at the lower level ($H = 19$ cm) the velocity profile remains nearly unchanged at the time step $t = 87$ s (Fig. 10), and only slight acceleration of the material for this level can be seen at the next time step 107 s (Fig. 11). Flow remains nearly symmetrical at this location and for the time $t = 87$ s, but some disturbance appears at the next time step (Fig. 11).

The last figure of the sequence (Fig. 12) shows a velocity profile obtained for the final stage of the process ($t = 154$ s). There is only one profile available for the lower level ($H = 19$ cm). It depicts an irregular avalanche type flow with strong asymmetry of the vertical velocity component. In fact most of the material slides along the side walls converging into the outlet (comp. Fig. 3e, f).

The transient changes of the flow pattern are illustrated in Fig. 13, where velocity profiles measured at the lower location $H = 19$ cm are collected for three time steps. It can be found that all three velocity profiles have a very similar shape, that indicates the same character of the flow in this period of time. Velocities reach their maximum values about 4 mm/s at the axis of symmetry of the model. A slight disturbance of flow symmetry is only present at the time step 45 s.

In this experimental analysis free gravitational discharge of a granular material (amaranth seed) is presented. The observed evolution of the plug flow zone can be deduced from Fig. 14, where the height of the plug flow as a function of time is shown. After opening the outlet a plug flow zone rapidly forms in the material and reaches the height of the packed material during the first 10 s after beginning of the flow. Till about 170 s of the flow, the evolution of the plug flow zone is represented by a slightly concave line. Evolution of the plug flow zone in the last phase of the flow relates almost to the linear relation.

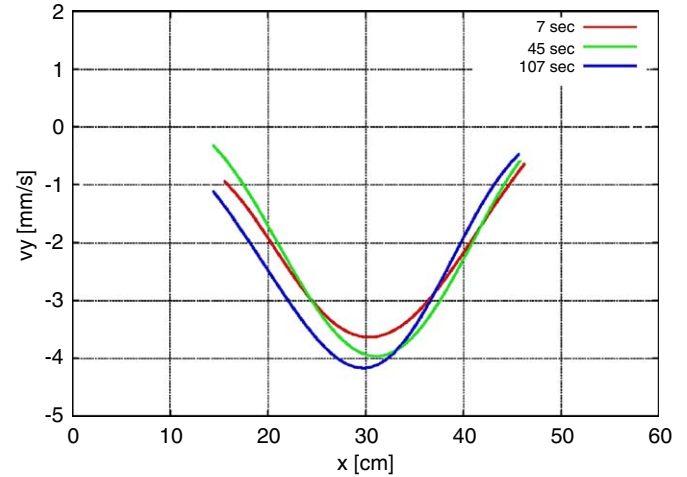


Fig. 13. Velocity profiles of the vertical component V_y for the location $H = 19$ cm measured at time steps 7, 45, and 107 s.

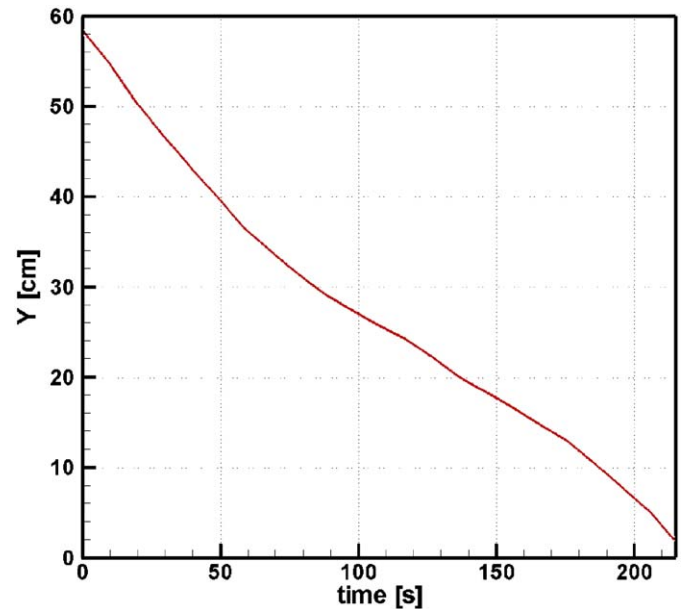


Fig. 14. Evolution of the height of plug flow zone measured in the symmetry axis.

As it was aforementioned, the discharge flow rate was measured using a digital scale before DPIV experiments were done. The total discharge time for amaranth seed was found equal 234 s. For the first 150 s the mass discharge rate was constant and equal 74.3 g/s. After this time, the discharge rate rapidly decreased to the value of 58.3 g/s at 180 s, and 45.0 g/s at 210 s. For the material density equal 832.5 kg/m^3 it corresponds to the volumetric discharge rates of 89.3, 70.1, and $54.1 \text{ cm}^3/\text{s}$, respectively. The abrupt decrease of the discharge rate can be explained by the fact that material in the model had considerably lower bulk density in the later phase of the flow. This observation is confirmed by independent measurements of the volumetric flow rate (comp. Fig. 15).

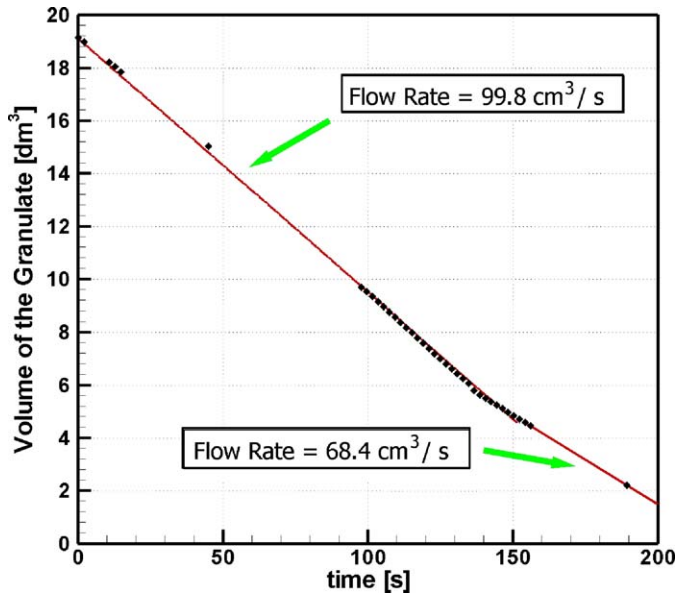


Fig. 15. Volumetric discharge flow rate for amaranth seed calculated from the images of the material in the model. Inclination of lines fitted to the experimental data indicates that the initial flow rate of $99.8 \text{ cm}^3/\text{s}$, decreases to about $68.4 \text{ cm}^3/\text{s}$ after 130 s.

To verify the accuracy of these measurements, several images of the seed flow collected during the experiments were evaluated and the areas filled with the material were used to calculate its volume. This image processing procedure is very reliable and permits to track instantaneous flow rate with accuracy better than 1%. Fig. 15 shows the results of the evaluation. The points showing the calculated volume of the material indicate almost the linear variation until about 150 s. This flow regime was approximated by linear regression shown in Fig. 15. The slope of the line indicates the flow rate equal $99.8 \text{ cm}^3/\text{s}$. After about 130 s the flow rate abruptly diminishes and is equal to approximately $68.4 \text{ cm}^3/\text{s}$. This behaviour confirms tendency noticed by the direct measurements of the discharge rate. The evaluated flow rate values are generally in accordance with the direct, weight-based measurements. The observed differences, mainly in the initial flow rate, can be due to the differences in the packing ratio of the material. It must be also emphasised, that our flow observations are limited to the wall vicinity only. One may expect that assumption of ideal two-dimensional flow can be violated and calculated material volume needs correction. To verify such possibility a three-dimensional imaging of the material interface is necessary.

5. Conclusions

In this paper an application of the DPIV technique to the analysis of flow evolution in a densely packed cohesionless material in a converging hopper is shown. This analysis allowed to evaluate the velocity of vectors for each point of the flow. The DPIV technique appears to be a sufficient diagnostic tool to investigate quasi two-dimensional granular flows. It gave us possibility to quantify flow regions, detect a radial veloc-

ity field, shear zones, and to measure transient variation of the velocity profiles at selected heights of the model. Accuracy of DPIV measurements allows to obtain velocity gradients inside the flowing zone. However, evaluation of hopper wall stresses is still a challenging task. The velocity of the granular material near the wall is equal or close to zero and cannot be used to calculate the wall stresses. The velocity gradients measured on the boundary of the stagnant zone could offer useful values for calculating wall stresses. Such evaluation, combined with the stresses measured at the wall by electrical transducers (Ostendorf and Schwedes, 2004), could offer a possibility to verify theoretical descriptions of mechanical properties of granular media in converging hoppers.

Acknowledgements

The authors express their great gratitude to the referees for suggestions which led to an improvement of the original manuscript. Many thanks to Professor Zenon Mroz from the IPPT PAN and Professor Andrew Drescher of the University of Minnesota for their valuable discussions and advices. We are also indebted to Dr. Marek Słodowski from the IPPT PAN for his assistance in some experiments. The work was accomplished in the framework of EU Thematic Network PIVNET2. The first author also acknowledges the financial support both of the Grant G/IIB/1/06 from the Polish Government and the DuPont company.

References

- Blair-Fish, P.M., Bransby, P.L., 1973. Flow patterns and wall stresses in a mass-flow bunker. *Journal of Engineering for Industry* 95, 17–26.
- Böhrnsen, J.U., Antes, H., Ostendorf, M., Schwedes, J., 2004. Silo discharge: measurement and simulation of dynamic behaviour in bulk solids. *Chemical Engineering and Technology* 27, 71–76.
- Cleaver, J.A.S., Nedderman, R.M., 1993a. Theoretical predictions of stress and velocity profiles in conical hoppers. *Chemical Engineering Science* 48, 3696–3702.
- Cleaver, J.A.S., Nedderman, R.M., 1993b. The measurement of velocity distributions in conical hoppers. *Chemical Engineering Science* 48, 3703–3712.
- Drescher, A., 1991. *Analytical Methods in Bin-load Analysis*, vol. 36, Development in Civil Engineering. Elsevier, Amsterdam.
- Drescher, A., Ferjani, M., 2004. Revised model for plug/funnel flow in bins. *Powder Technology* 141, 44–54.
- Drescher, A., Cousens, T.W., Bransby, P.L., 1978. Kinematics of the mass flow of granular material through a plane hopper. *Geotechnique* 28, 27.
- Dosekun, R., 1980. The flow of granular materials. Ph.D. Thesis. University of Cambridge.
- Hill, R., 1950. *The Mathematical Theory of Plasticity*. Clarendon Press, Oxford.
- Horne, R.M., Nedderman, R.M., 1978. Stress distributions in hoppers. *Powder Technology* 19, 243–254.
- Jenike, A.W., 1961. Gravity Flow of Bulk Solids. University of Utah Engineering Experiment Station, Bulletin, vol. 108, USA.
- Jenike, A.W., 1964. Storage and Flow of Solids. University of Utah Engineering Experiment Station, Bulletin, vol. 123, USA.
- Johanson, J.R., Jenike, A.W., 1962. Stress and velocity fields in gravity flow of bulk solids. University of Utah Engineering Experiment Station, Bulletin, vol. 116, USA.
- Kvapil, R., 1959. *Theorie der Schüttgutbewegung*. VEB Verlag Technik, Berlin.

- Langston, P.A., Tuzun, U., Heyes, D.M., 1996. Distinct element simulation of interstitial air effects in axially symmetric granular flows in hoppers. *Chemical Engineering Science* 51, 873–891.
- Langston, P.A., Nikitidis, M.S., Tuzun, U., Heyes, D.M., Spyrou, N.M., 1997. Microstructural simulation and imaging of granular flows in two- and three-dimensional hoppers. *Powder Technology* 94, 59–72.
- Lee, J., Cowin, S.C., Templeton, J.S., 1974. An experimental study of the kinematics of flow through hoppers. *Transactions of the Society of Rheology* 18, 247–269.
- Litwiniszyn, J., 1963. The model of a random walk of particles adopted to researches on problem of mechanics of loose media. *Bulletin de l'Academie Polonaise des Sciences* 11, 61–70.
- Lueptow, R.M., Akonur, A., Shinbrot, T., 2000. PIV for granular flows. *Experiments in Fluids* 28, 183–186.
- Moreea, S.B.M., Nedderman, R.M., 1996. Exact stress and velocity distributions in a cohesionless material discharging from a conical hopper. *Chemical Engineering Science* 51, 3931–3942.
- Mróz, Z., Szymański, Cz., 1971. Gravity flow of a granular material in a converging channel. *Arch. Mech.* 23, 897–917.
- Mullins, W.W., 1972. Stochastic theory of particle flow under gravity. *Journal of Applied Physics* 43, 665–677.
- Mullins, W.W., 1979. Critique and comparison of two stochastic theories of gravity-induced particle flow. *Powder Technology* 23, 115–119.
- Nedderman, R.M., 1988. Measurement of the velocity profile in a granular material discharging from a conical hopper. *Chemical Engineering Science* 43, 1507–1516.
- Nedderman, R.M., 1995. The use of the kinematic model to predict the development of the stagnant zone boundary in the batch discharge of a bunker. *Chemical Engineering Science* 50, 959–965.
- Nedderman, R.M., Tüzün, U., 1979. A kinematic model for the flow of granular materials. *Powder Technology* 22, 243–253.
- Nguyen, T.V., Brennen, C., Sabersky, R.H., 1979. Gravity flow of granular materials in conical hoppers. *Journal of Applied Mechanics-Transactions of the ASME* 46, 529–535.
- Ooi, J.Y., Chen, J.F., Rotter, J.M., 1998. Measurement of solids flow patterns in a gypsum silo. *Powder Technology* 99, 272–284.
- Ostendorf, M., Schwedes, J., 2004. Application of optical measurement techniques on the investigation of bulk solids flow behaviour in silos. *International Congress for Particle Technology, Partec 2004, Nurnberg, Germany, 16–18 March*
- Pariseau, W.G., 1969. Discontinuous velocity fields in gravity flows of granular materials through slots. *Powder Technology* 3, 218–226.
- Pitman, E.B., 1986. Stress and velocity fields in two- and three-dimensional hoppers. *Powder Technology* 47, 219–231.
- Polderman, H.G., Scott, A.M., Boom, J., 1985. Solids stresses in bunkers with inserts. *Int. Chem. Engng. Symp. Ser.* 91, 227–240.
- Prager, W., Hodge, P.G., 1968. *Theory of Perfectly Plastic Solids*. Dover Publications, New York.
- Quenot, G.M., Pakleza, J., Kowalewski, T.A., 1998. Particle image velocimetry with optical flow. *Experiments in Fluids* 25, 177–189.
- Salençon, J., 1977. *Application of the Theory of Plasticity in Soil Mechanics*. Wiley, New York.
- Sielamowicz, I., Kowalewski, T.A., 2004. DPIV technique in modelling granular material flows in a model of silo made of Plexiglas. *International Congress for Particle Technology, Partec 2004, Nurnberg, Germany, 16–18 March*.
- Sielamowicz, I., Blonski, S., Kowalewski, T.A., 2005. Optical technique DPIV in measurements of granular material flows, Part 1 of 3-plane hoppers. *Chemical Engineering Science* 60, 589–598.
- Steingart, D.A., Evans, J.W., 2005. Measurements of granular flows in two-dimensional hoppers by particle image velocimetry. Part I: experimental method and results. *Chemical Engineering Science* 60, 1043–1051.
- Tüzün, U., Nedderman, R.M., 1982. Investigation of the flow boundary during steady-state discharge from a funnel-flow bunker. *Powder Technology* 31, 27–43.
- Tüzün, U., Houlisby, G.T., Nedderman, R.M., Savage, S.B., 1982. The flow of granular materials-II; velocity distributions in slow flow. *Chemical Engineering Science* 37, 1691–1709.
- Walker, D.M., 1966. An approximate theory for pressures and arching in hoppers. *Chemical Engineering Science* 21, 975–997.
- Waters, A.J., Drescher, A., 2000. Modeling plug flow in bins/hoppers. *Powder Technology* 113, 168–175.
- Watson, G.R., Rotter, J.M., 1996. A finite element kinematic analysis of planar granular solids flow. *Chemical Engineering Science* 51, 3967–3978.